Journal of Visualized Experiments

Assessment of acute wound healing using the dorsal subcutaneous polyvinyl alcohol sponge implantation and excisional tail skin wound models.
--Manuscript Draft--

Article Type:	Invited Methods Article - JoVE Produced Video
Manuscript Number:	JoVE60653R1
Full Title:	Assessment of acute wound healing using the dorsal subcutaneous polyvinyl alcohol sponge implantation and excisional tail skin wound models.
Section/Category:	JoVE Immunology and Infection
Keywords:	wound; Wound healing model; fibrosis; surgery; trauma; mouse; inflammation; Innate Immune Response
Corresponding Author:	Amanda Jamieson Brown University Providence, Rhode Island UNITED STATES
Corresponding Author's Institution:	Brown University
Corresponding Author E-Mail:	amanda_jamieson@brown.edu
Order of Authors:	Meredith J. Crane
	William L. Henry
	Holly L. Tran
	Jorge E. Albina
	Amanda M. Jamieson
Additional Information:	
Question	Response
Please indicate whether this article will be Standard Access or Open Access.	Standard Access (US$2,400)
Please indicate the **city, state/province, and country** where this article will be **filmed**. Please do not use abbreviations.	Providence, RI USA

1 **TITLE:**
2 **Assessment of Acute Wound Healing using the Dorsal Subcutaneous Polyvinyl Alcohol Sponge**
3 **Implantation and Excisional Tail Skin Wound Models**
4

5 **AUTHORS AND AFFILIATIONS:**
6 Meredith J. Crane[1], William L. Henry[1], Jr., Holly L. Tran[1], Jorge E. Albina[2], Amanda M. Jamieson[1]
7

8 [1]Department of Molecular Microbiology & Immunology, Brown University, Providence, RI, USA
9 [2]Division of Surgical Research, Department of Surgery, Rhode Island Hospital and The Warren
10 Alpert School of Medicine of Brown University, Providence RI, USA
11

12 **Corresponding Author:**
13 Amanda M. Jamieson   (Amanda_Jamieson@brown.edu)
14

15 **Email Addresses of Co-authors:**
16 Meredith J. Crane   (meredith_crane@brown.edu)
17 William L. Henry, Jr.   (william_henry@brown.edu)
18 Holly L. Tran   (holly_tran@brown.edu)
19 Jorge E. Albina   (Jorge_Albina@brown.edu)
20

21 **KEYWORDS:**
22 wound, wound healing model, fibrosis, surgery, trauma, mouse, inflammation, innate immune
23 response
24

25 **SUMMARY:**
26 Here, two murine wound healing models are described, one designed to assess cellular and
27 cytokine wound healing responses and the other to quantify the rate of wound closure. These
28 methods can be used with complex disease models such as diabetes to determine mechanisms
29 of various aspects of poor wound healing.
30

31 **ABSTRACT:**
32 Wound healing is a complex process that requires the orderly progression of inflammation,
33 granulation tissue formation, fibrosis, and resolution. Murine models provide valuable
34 mechanistic insight into these processes; however, no single model fully addresses all aspects of
35 the wound healing response. Instead, it is ideal to use multiple models to address the different
36 aspects of wound healing. Here, two different methods that address diverse aspects of the
37 wound healing response are described. In the first model, polyvinyl alcohol sponges are
38 subcutaneously implanted along the mouse dorsum. Following sponge retrieval, cells can be
39 isolated by mechanical disruption, and fluids can be extracted by centrifugation, thus allowing
40 for a detailed characterization of cellular and cytokine responses in the acute wound
41 environment. A limitation of this model is the inability to assess the rate of wound closure. For
42 this, a tail skin excision model is utilized. In this model, a 10 mm x 3 mm rectangular piece of tail
43 skin is excised along the dorsal surface, near the base of the tail. This model can be easily
44 photographed for planimetric analysis to determine healing rates and can be excised for

45 histological analysis. Both described methods can be utilized in genetically altered mouse strains,
46 or in conjunction with models of comorbid conditions, such as diabetes, aging, or secondary
47 infection, in order to elucidate wound healing mechanisms.
48
49 **INTRODUCTION:**
50 There are many murine model systems available to examine wound healing processes, each
51 possessing specific advantages and limitations[1,2]. The following methods present two murine
52 wound models, each of which addresses a particular aspect of the wound healing response, and
53 which can be used to identify the cause and effect of perturbations in the response to injury. The
54 process of wound healing occurs in distinct phases. The first phase is inflammatory, characterized
55 by the rapid influx of platelets, neutrophils, and monocytes/macrophages, as well as the
56 production of proinflammatory cytokines and chemokines. Following resolution of inflammation,
57 the environment transitions to a more reparative state with the induction of profibrotic and
58 proangiogenic cytokines and growth factors. Granulation tissue is deposited and neovessels form
59 with the migration of myofibroblasts, fibroblasts, epithelial cells, and endothelial cells. In the final
60 stages, the provisional extracellular matrix is remodeled, and scar formation and wound closure
61 proceeds[2-8].
62
63 No single murine model provides a system to study all stages of wound healing[2]. Here, two
64 surgical wound models are described: one elucidates acute cellular and cytokine wound healing
65 responses, and the other allows for the assessment of wound closure as well as histological
66 analyses. These two methods may be employed in a complementary fashion to assess the effects
67 of a perturbation or comorbidity on different aspects of the wound healing response. The dorsal
68 subcutaneous implantation of polyvinyl alcohol (PVA) sponges is a system that has been used in
69 rodent models for decades to elucidate numerous aspects of cellular and granulation tissue
70 responses[9-24]. This approach allows for the retrieval of cytokine-rich wound fluids and cellular
71 infiltrates. In this model, 1 cm x 1 cm x 0.5 cm pieces of PVA sponge are placed into subcutaneous
72 pockets through a 2 cm incision made at the posterior dorsal midline. The incision is closed with
73 surgical clips, and the sponges can be retrieved at later time points for cell and fluid isolation.
74 The cellular and cytokine milieu of isolated sponges reflects the normal stages of acute wound
75 healing up to about 14 days postimplantation. At later time points the model is more
76 advantageous for studying granulation tissue formation and the foreign body response[1]. With
77 this system, it is possible to isolate $>10^6$ cells, which offers a distinct advantage for phenotypic
78 and functional assays and RNA isolation, over isolating cells from other biopsy-based
79 methods[1,22,23,25,26].
80
81 The rate of wound closure is determined using the tail skin excision model. In this model, as
82 initially described by Falanga et al. and reported by others[27-30], a 1 cm x 0.3 cm full thickness
83 section of tail skin is removed near the base of the tail. The wound area is easily visualized and
84 can be measured over time. Alternatively, tail tissue can be isolated for histological analysis. This
85 approach can be used as an alternative to or in conjunction with the well-established dorsal
86 punch biopsy method. The primary distinctions between these two models are the rate of wound
87 closure, the presence or absence of fur, and the skin structure[2,31,32]. Tail skin wounds offer a
88 longer timeframe in which to assess wound closure, as it takes approximately 21 days for full

89 closure to occur. This is opposed to unsplinted dorsal punch biopsies, which heal much faster
90 (~7–10 days), primarily by contraction due to the action of the panniculus carnosus. Splinted
91 dorsal punch biopsies heal more slowly and diminish the effects of contractile healing, but rely
92 on the presence of a foreign body to restrict contractile-based mechanisms[1,2,27,30,31,33].
93
94 The described wound models are informative for understanding normal wound healing processes
95 in the absence of perturbation. While the healing of rodent skin differs in very significant ways
96 from human skin, including loose structure, reliance on contractile healing, and other anatomical
97 differences, the murine system offers certain advantages for mechanistic and screening studies.
98 Foremost among these is the availability of inbred strains and genetic mutants, genetic
99 tractability, and lower cost. Mechanistic insight gained from murine studies can be translated to
100 complex animal models that more closely mimic human skin healing, such as the porcine
101 system[2,31].
102
103 In addition to examining wound healing responses in the steady state, these models can be
104 combined with comorbid conditions to understand the basis of wound healing defects at the
105 cellular, cytokine, and gross tissue level. It is in this particular setting that the two models can be
106 used in concert to assess the effects of a particular comorbid condition, such as postoperative
107 pneumonia, on both the acute cellular wound healing response and the rate of wound closure[30].
108
109 **PROTOCOL:**
110 All animal studies described here were approved by the Brown University Institutional Animal
111 Care and Use Committee and carried out in accordance with the Guide for the Care and Use of
112 Animals of the National Institutes of Health.
113
114 **1. Subcutaneous implantation of PVA sponges**
115
116 1.1. Use scissors to cut sheets of PVA sponge into 8 mm x 8 mm x 4 mm pieces. Rehydrate the
117 pieces of PVA sponge by submerging them in sterile 1x PBS in a beaker.
118
119 1.2. Autoclave the sponges in 1x PBS to sterilize, and cool completely. Store autoclaved sponges
120 in sterile 1x PBS at 4 °C.
121
122 1.3. Prior to performing surgical implantation, aliquot the necessary number of sponges into a
123 sterile culture dish under sterile conditions in a laminar flow hood. Store the extra sponges in
124 sterile 1x PBS at 4 °C for future use. Ensure that the sponges swell to 1 cm x 1 cm x 0.5 cm after
125 rehydration. An image of dehydrated PVA sponges is shown in **Figure 1A**.
126
127 NOTE: To maintain the sterility of the surgical site, the PVA sponge implantation procedure
128 requires one individual to handle the mouse and prepare the surgical site, and a second person
129 to perform the implantation.
130
131 1.4. Anesthetize an 8–12 week-old male C57BL/6J mouse by intraperitoneal injection of 80 mg/kg
132 ketamine. Confirm the depth of anesthesia by the loss of a pedal reflex. Prepare the surgical site

133 by removing the hair along the dorsum with clippers. Using sterile gauze, apply povidone-iodine
134 solution to the shave area 2x, followed by 70% ethanol.

136 1.5. Place the mouse on sterile surgical drapes. Place a heated pad below the surgical drapes to
137 maintain the mouse's core temperature.

139 1.6. Wear sterile surgical gloves for performing the surgery. Pull the dorsal skin away from the
140 underlying tissue with forceps, and using sterile surgical scissors, make a 2 cm incision along the
141 dorsal midline approximately 2 cm anterior to the base of the tail. While holding the incision open
142 with sterile forceps, use sterile curved, blunt-tipped surgical scissors to form a subcutaneous
143 pocket along the dorsum in one of the positions indicated in **Figure 1B**.

145 1.7. Continue to use forceps to lift the skin away from the underlying tissue. Using sterile surgical
146 scissors, gently squeeze one PVA sponge in the culture dish to remove excess PBS. Pick up the
147 PVA sponge by one corner using sterile surgical scissors and, leading with the corner held by the
148 scissors, place the sponge into the subcutaneous pocket formed in step 1.4.

150 1.8. Repeat this process 5x, placing a total of six sponges into subcutaneous pockets as shown in
151 **Figure 1B**.

153 1.9. Pinch the incised dorsal skin together with sterile forceps and close the incision with two
154 stainless steel wound clips.

156 1.10. Use a new set of sterile surgical instruments for each mouse. Alternatively, use a bead
157 sterilizer to sterilize instruments between mice.

159 **2. Isolation of fluids from PVA sponges**

161 2.1. To assess the acute wound cytokine milieu, isolate sponges between 1–14 days
162 postimplantation.

164 2.2. Prepare a fluid collection tube by nesting the barrel of a 5 mL syringe into a 16 mL culture
165 tube.

167 2.3. Euthanize a mouse with implanted PVA sponges by CO_2 asphyxiation followed by cervical
168 dislocation.

170 2.4. Remove the surgical staples and open the incision with toothed forceps. Use scissors to
171 extend the incision along the dorsal midline.

173 2.5. Using forceps, extract one sponge from its subcutaneous pocket and transfer it to the
174 prepared syringe barrel, being careful to minimize pressure to the sponge. Disassociate any
175 connective tissue that remains adhered to the surface of the sponge. Use scissors to dissect the
176 sponge from the surrounding tissue if necessary. Repeat the sponge removal process with the

177   remaining sponges. Place the tube containing the sponges on ice.
178
179   2.6. To isolate the wound fluid, centrifuge the culture tube containing the 5 mL syringe with the
180   sponges at 700 x g for 10 min.
181
182   2.7. After the centrifugation, discard the syringe and the sponges. The wound fluid will have
183   collected in the 16 mL culture tube. A representative image of fluid collected from a day 7 wound
184   is shown in **Figure 1D**. Transfer the wound fluid to a clean tube for long-term storage at -80 °C.
185
186   **3. Isolation of cells from PVA sponges**
187
188   3.1. To assess the acute wound healing cellular milieu, collect sponges between 1–14-days post-
189   sponge implantation. Sponges obtained from a wound 7 days after implantation are shown in
190   **Figure 1E**.
191
192   3.2. Prepare collection medium containing 1x HBSS (+calcium/+magnesium/–phenol red)
193   supplemented with 1% FBS, 1% HEPES, and 1% penicillin-streptomycin.
194
195   3.3. Aliquot 5 mL of HBSS collection medium into a 15 mL conical tube.
196
197   3.4. Extract the PVA sponges from euthanized mice as described in 2.2–2.4. Place the sponges
198   into the conical tube containing 5 mL of HBSS collection medium.
199
200   3.5. Transfer the sponges and the HBSS collection medium to an 80 mL blender bag by pouring.
201   Hang the blender bag from the hatch of the paddle blender, positioned so that the paddles strike
202   the sponges and media. Adjust the settings of the paddle blender to run on high for 60 s. Press
203   start.
204
205   3.6. Transfer the media from the blender bag back to the 15 mL conical tube with a pipette,
206   leaving the sponges behind in the bag. Squeeze the sponges to thoroughly release the media.
207   Adjust the settings of the paddle blender to run for 30 s on high. Add 5 mL of media to the blender
208   bag and repeat the stomaching process 2x for a total of three sponge washes.
209
210   3.7. Centrifuge the conical tube at 250 x g for 5 min. A red pellet of cells and red blood cells will
211   be visible at the bottom of the conical tube after centrifugation.
212
213   3.8. Discard the supernatant and perform a red blood cell lysis: add 900 µL of dH$_2$O to the cell
214   pellet and pipette to mix. Neutralize with 100 µL of 10x PBS. Add 4 mL of 1x PBS to the tube to
215   fully neutralize the lysis, then centrifuge at 250 x g for 5 min.
216
217   NOTE: The lysis step should be brief; leaving the water in contact with the cells for more than 3–
218   5 s could result in lysis of non-red blood cells.
219
220   3.9. After centrifugation, a white cell pellet containing wound cells devoid of red blood cells will

221 be present at the bottom of the conical tube. Discard the supernatant and resuspend the cell
222 pellet in the desired medium for downstream analyses.
223
224 **4. Optional flow cytometry analysis of innate leukocytes isolated from PVA sponge wounds**
225
226 4.1. Resuspend 0.5–1 x 10^6 wound cells in 25 µL of a 2x solution of blocking antibody containing
227 10 µg/mL anti-CD16/CD32 FcRγII/III antibody diluted in 1x PBS + 1% BSA.
228
229 NOTE: All antibodies should be titrated to determine optimal concentrations for flow cytometry
230 analysis.
231
232 4.2. Incubate the cells with blocking antibody for 10 min on ice.
233
234 4.3. Make a 2x master mix of antibodies containing 2.5 mg/mL of PerCP-eFluor710-Ly6G, 5
235 mg/mL of FITC-Ly6C, APC-Fire750-CD45.2, APC-R700-Siglec-F, and 10 mg/mL of eFluor660-F4-80
236 diluted in 1x PBS + 1% BSA. Directly add 25 µL of the antibody cocktail to the cells incubating in
237 blocking antibody.
238
239 4.4. Incubate the cells for 20 min on ice, protected from light.
240
241 4.5. Wash the cells 2x with 1x PBS.
242
243 4.6. Make a master mix of amine-reactive fixable viability dye-eFluor506 diluted 1:1,000 in 1x
244 PBS. Resuspend the cell pellet in 50 µL of the viability dye solution.
245
246 NOTE: Serum must be excluded from the fixable viability step, as it will prevent binding of the
247 dye to endogenous proteins. Incubate the cells for 20 min on ice, protected from light.
248
249 4.7. Wash the cells 2x with 1x PBS. Resuspend the cell pellet in 50 µL of 1% paraformaldehyde.
250
251 4.8. Incubate the cells with 1% paraformaldehyde for 15 min on ice, protected from light.
252
253 4.9. Wash the cells 1x with 1x PBS and resuspend the pellet in 1x PBS for flow cytometric analysis.
254
255 **5. Tail skin excision**
256
257 5.1. Anesthetize an 8–12 week-old male C57BL/6J mouse by intraperitoneal injection of 80 mg/kg
258 of ketamine. Confirm the depth of anesthesia by the loss of a pedal reflex.
259
260 5.2. Prepare the surgical site on the tail of the anesthetized mouse by using sterile gauze to apply
261 povidone-iodine solution 2x, followed by one application of 70% ethanol.
262
263 5.3. Define a 10 mm x 3 mm section on the dorsal surface of the tail, 10 mm from the base of the
264 tail (**Figure 1C**) using a permanent marker to trace from a premade template.

265

266 5.4. Cover the anesthetized mouse with sterile surgical drapes.

267

268 5.5. Wear sterile surgical gloves to perform the surgical procedures. With a sterile scalpel blade,
269 make a full thickness incision along the right, bottom, and left edges of the wound area.

270

271 5.6. Using sterile forceps, peel the excised skin away from the tail, and use sterile surgical scissors
272 to cut away the top edge of the wound area.

273

274 5.7. Apply pressure with sterile gauze to stop bleeding.

275

276 5.8. Apply a spray barrier film to the wound bed.

277

278 5.9. Photograph the wounds from a fixed distance at regular time intervals. Analyze photographs
279 by planimetric analysis to determine wound area measurements. Alternatively, use calipers to
280 obtain wound length and width measurements.

281

282 **REPRESENTATIVE RESULTS:**
283 **Systemic inflammatory response following PVA sponge implantation**
284 The PVA sponge implantation surgery generated a systemic inflammatory response, as
285 demonstrated by the induction of IL-6 in the plasma 1 day after wounding (**Figure 2A**). Other
286 proinflammatory cytokines including TNF-α and IL-1β, as well as an array of chemokines including
287 CCL2 and CXCL1 were induced systemically in the first 7 days post-PVA sponge implantation, and
288 have been described elsewhere[26,30].

289

290 **Isolation of cells and fluids from PVA sponge wounds**
291 The primary advantage of the PVA sponge wound model is the ability to recover enough cells for
292 phenotypic and functional analyses of the acute cellular wound healing response. The number of
293 cells that can be recovered from PVA sponge wounds increases over time, from approximately 2
294 x 10^6 cells per six sponges on wound day 1 x 10^6 to 8 x 10^6 cells on wound day 7 (**Figure 2B**). The
295 cell number continues to increase beyond day 7. It is not recommended to continue this model
296 beyond ~14 days because the sponges become fully encapsulated by collagen and the system
297 transitions from modeling an acute wound healing response to modeling a foreign body
298 granuloma[1,22,23,25,26]. Neutrophils, monocytes, and macrophages were the primary cellular
299 infiltrate in PVA sponge wounds. Neutrophils predominated the wound cellular milieu one day
300 after wounding, as assessed by flow cytometric analysis (**Figure 2C**). Monocytes and monocyte-
301 derived macrophages accumulated within 3 days post-sponge implantation, and the three cell
302 populations increased in number over time (**Figure 2C**). A representative flow cytometry gating
303 strategy to identify neutrophil, monocyte, and macrophage populations is shown in **Figure 2D**.
304 After excluding cell doublets using FSC-H and SSC-H parameters (**Figure 2D**, **i** and **ii**), non-viable
305 cells were excluded using an amine-reactive fixable viability dye (shown here) or a nucleic acid
306 dye (e.g., sytox or propidium iodide) (**Figure 2D**, **iii**). Residual cellular debris not removed by the
307 prior gating steps was then excluded using FSC-A and SSC-A parameters (**Figure 2D**, **iv**).
308 Hematopoietic cells comprised the majority of PVA sponge wound cells and were identified by

309 CD45 expression (**Figure 2D**, **v**). Neutrophils were identified as Ly6G⁺Siglec-F⁻ (**Figure 2D**, **vi**).
310 Siglec-F⁺ cells were primarily eosinophils (**Figure 2D**, **vii**). Gating on Ly6G⁻Siglec-F⁻ cells,
311 monocytes/macrophages were identified as F4/80⁺ cells (**Figure 2D**, **viii**). F4/80⁺ cells could be
312 further fractionated by Ly6C expression to distinguish Ly6C^{hi} inflammatory monocytes (**Figure 2D**,
313 **ix**) and Ly6C^{low} monocyte-derived macrophages (**Figure 2D**, **x**)[26].
314
315 The ability to measure cytokines and other wound soluble factors is another advantage to the
316 PVA sponge wound model. It is possible to extract up to 100 µL of fluid per sponge. Extracted
317 fluids are suitable for a variety of downstream assays. The detection of cytokines and chemokines
318 in early and late wound fluids by ELISA or bead-based multiplex immunoassays have been
319 reported elsewhere[26,30]. It is possible to obtain both cells and fluids from the same wound. To do
320 this, it is recommended to isolate three sponges from one side of the dorsal midline for cell
321 isolation and 3 sponges from the opposite side of the dorsal midline for fluid extraction.
322
323 **Assessment of wound closure using the tail skin excision model**
324 The excisional tail skin model provides an alternative to the dorsal skin punch biopsy method to
325 study slow wound closure in firm skin lacking dense fur. Example images of tail skin wounds at 1,
326 7, and 15 days post-excision are shown in **Figure 3A**. Wound closure could be quantified by
327 measuring the area of the wound bed over time. The day 7 and day 15 wound bed areas were
328 approximately 70% and 35%, respectively, of the day 1 wound area (**Figure 3B**). Full wound
329 closure required approximately 28 days. The tail skin wound could also be observed in cross
330 section by histological analysis. **Figure 3C** and **Figure 3D** show representative images of H&E and
331 Masson's Trichrome-stained tail cross sections, respectively. The lateral margins of the excised
332 skin are indicated by arrowheads on the dorsal surface of the tail.
333
334 **FIGURE AND TABLE LEGENDS:**
335
336 **Figure 1: Schematic of murine wound healing models.** (**A**) Side (left) and top (right) view of
337 dehydrated PVA sponges measuring 8 mm x 8 mm x 0.4 mm. (**B**) Illustration of a mouse
338 demonstrating the placement of the dorsal midline incision (central red line) and six 1 cm x 1 cm
339 x 0.5 cm PVA sponges in subcutaneous pockets. (**C**) Schematic demonstrating the size and
340 placement of an excisional skin wound (10 mm x 3 mm red rectangle) on the dorsal surface of
341 the tail. (**D**) Wound fluid isolated from three sponges that were retrieved from the subcutaneous
342 space 7 days after implantation. (**E**) The appearance of sponges retrieved from the wound 7 days
343 after implantation.
344
345 **Figure 2: The systemic and cellular response to PVA sponge implantation.** (**A**) A time course of
346 IL-6 levels in the plasma demonstrates that PVA sponge implantation induced a systemic
347 inflammatory response. The concentration of IL-6 was measured using a multiplex bead-based
348 immunoassay. (**B**) The number of cells isolated from PVA sponges wound increased over time.
349 (**C**) A time course demonstrates the accumulation of neutrophils, monocytes, and monocyte-
350 derived macrophages in PVA sponge wounds over time. (**D**) A representative gating strategy of
351 cells isolated from PVA sponge wounds demonstrates how to identify leukocyte subsets by flow
352 cytometric analysis. Gates are defined as follows: (**i** and **ii**) doublet exclusion, (**iii**) dead cell

353　exclusion using an amine-reactive fixable viability dye, (**iv**) debris exclusion by FSC-A and SSC-A,
354　(**v**) $CD45^+$ hematopoietic cells, (**vi**) $Ly6G^+$ neutrophils, (**vii**) Siglec-F^+ eosinophils, (**viii**) $Ly6G^-$Siglec-
355　F^- $F4/80^+$ monocytes/macrophages, (**ix**) $F4/80^+Ly6C^{hi}$ monocytes, and (**x**) $F4/80^+Ly6C^{low}$
356　macrophages. Gates were placed according to fluorescence-minus one (FMO) controls. The data
357　shown in **A**–**C** are the mean ± SEM, n = 6–10 mice per group in (**A**), n = 8–9 mice in (**B**), and n =
358　6–8 mice in (**C**). All data are combined from 2–3 independent experiments.
359
360　**Figure 3: Assessment of excisional tail skin wound healing.** (**A**) Representative photographs of
361　excisional tail skin wounds taken 1, 7, and 15 days post-wounding. (**B**) The rate of closure of
362　excisional tail skin wounds. Wounds were photographed every other day. Image processing
363　software was used to trace the wound bed margins and calculate the wound area at indicated
364　time points. The wound area is presented as a fraction of the wound area measured on day 1.
365　Representative images of tail cross sections that were paraffin-embedded, sectioned, and stained
366　with (**C**) H&E or (**D**) Masson's Trichrome. The wound was located on the dorsal surface of the tail
367　cross section; lateral wound margins are indicated by arrowheads. The data shown in (**B**) are the
368　mean ± SEM, n = 8 mice per group. Data are combined from two independent experiments.
369
370　**DISCUSSION:**
371　This article describes two tractable murine wound models that allow for the assessment of the
372　acute wound healing response. The first method involves the surgical implantation of PVA
373　sponges in the dorsal subcutaneous space. This approach offers a distinct advantage over biopsy-
374　based wound models for studying the cellular wound healing response due to the large number
375　of cells and quantity of wound fluids obtained from the isolated sponges. For the successful
376　execution of this procedure, maintaining a sterile surgical field by thoroughly cleaning the skin
377　around the incision is imperative, as translocation of bacteria into the wound will significantly
378　alter the course of healing. Using the cell isolation method described here, it is possible to isolate
379　at least $1–10 \times 10^6$ cells from the PVA sponges, depending on the time of sponge extraction. The
380　majority of cells isolated from PVA sponge wounds are viable (**Figure 2D**). However, because it is
381　possible for dead cells to constitute up to ~20% of isolated wound cells after mechanical
382　disruption, it is highly recommended to use a viability stain when proceeding with flow
383　cytometry-based analyses. Cells isolated from PVA sponge wounds are primarily of
384　hematopoietic origin as determined by CD45 positivity (**Figure 2D**). The rapid accumulation of
385　neutrophils followed by monocytes and macrophages is consistent with the acute stages of
386　wound repair[3,4,34-38]. Isolated cells are suitable for downstream analyses including
387　immunophenotyping, cell sorting, culturing, RNA extraction, and a variety of functional assays.
388
389　The PVA sponge wound model also allows for the isolation of fluids, which is ideal for assessing
390　cytokine and growth factor responses in the acute wound environment. PVA sponge fluids are
391　suitable for testing by ELISA, bead-based multiplex immunoassay, and protein quantitation,
392　among others. Previous studies have demonstrated through cytokine and growth factor
393　measurement that the early wound environment is inflammatory in nature, with rapid induction
394　of IL-6, TNF-α, and IL-1β from days 1–3. The wound environment then transitions to a reparative
395　state with the later induction of pro-angiogenic and pro-fibrotic growth factors, including VEGF
396　and TGF-β[22,23,25,26,30].

397
398 While the PVA sponge implantation model is advantageous for studying acute wound cellular and
399 cytokine responses, one of its limitations is the inability to measure the rate or degree of healing.
400 Measurement of this aspect of wound healing may be required when assessing the effects of a
401 comorbid condition on various aspects of the wound healing response[30]. For this metric, biopsy-
402 based methods are preferred. Here, the tail skin excision model is presented. In this model, a full
403 thickness section of tail skin is excised from the dorsal surface of the tail. Again, maintaining a
404 sterile surgical field is important to avoid inoculating the wound bed. The use of a spray barrier
405 film or other wound covering is also recommended to avoid later wound infection. Older male
406 mice or aggressive strains require solo housing to avoid disruption of the wound. A particular
407 advantage of the tail as a site for studying wound healing is that it relies more on re-
408 epithelialization for closure, as described by others[27,32,33]. In addition to measuring the wound
409 bed area and performing histological analyses, others have reported its use in assessing the
410 efficacy of topical interventions in modulating the healing processes[33].
411
412 Each of the wound models described in these methods offer distinct advantages for
413 understanding wound repair processes in the steady state and in the presence of comorbidities.
414 Due to the wide availability of genetically altered strains of inbred mice, it is also possible to
415 manipulate the wound healing responses to answer mechanistic questions about the process.
416 Furthermore, these systems can be implemented in murine models of conditions associated with
417 poor wound healing including diabetes, aging, secondary infection, and others[30,36,39,40]. The
418 mechanistic insights gained from murine studies may then provide the basis for studying wound
419 healing in higher order animal models. Together, the PVA sponge implantation and excisional tail
420 skin wound models provide tractable and versatile systems to elucidate wound healing processes
421 under steady state and pathological conditions.
422

432

433 **DISCLOSURES:**
434 The authors have nothing to disclose.
435

436 **REFERENCES**
437 1.   Gottrup, F., Agren, M. S., Karlsmark, T. Models for use in wound healing research: a
438 survey focusing on in vitro and in vivo adult soft tissue. *Wound Repair and Regeneration:*
439 *Official Publication of the Wound Healing Society [and] the European Tissue Repair Society.* **8**
440 (2), 83–96 (2000).

441   2.   Elliot, S., Wikramanayake, T. C., Jozic, I., Tomic-Canic, M. A Modeling Conundrum:
442 Murine Models for Cutaneous Wound Healing. *Journal of Investigative Dermatology.* **138** (4),
443 736–740 (2018).
444   3.   Eming, S. A., Martin, P., Tomic-Canic, M. Wound repair and regeneration: Mechanisms,
445 signaling, and translation. *Science Translational Medicine.* **6** (265), 265sr6 (2014).
446   4.   Huber-Lang, M., Lambris, J. D., Ward, P. A. Innate immune responses to trauma. *Nature*
447 *Immunology.* **19** (4), 327–341 (2018).
448   5.   Novak, M. L., Koh, T. J. Phenotypic Transitions of Macrophages Orchestrate Tissue Repair.
449 *The American Journal of Pathology.* **183** (5), 1352–1363 (2013).
450   6.   Martins-Green, M., Petreaca, M., Wang, L. Chemokines and Their Receptors Are Key
451 Players in the Orchestra That Regulates Wound Healing. *Advances in Wound Care.* **2** (7), 327–
452 347 (2013).
453   7.   Guerrero-Juarez, C. F. et al. Single-cell analysis reveals fibroblast heterogeneity and
454 myeloid-derived adipocyte progenitors in murine skin wounds. *Nature Communications.* **10** (1),
455 650 (2019).
456   8.   Shook, B. A. et al. Myofibroblast proliferation and heterogeneity are supported by
457 macrophages during skin repair. *Science.* **362** (6417), eaar2971 (2018).
458   9.   Davidson, J. M. et al. Accelerated wound repair, cell proliferation, and collagen
459 accumulation are produced by a cartilage-derived growth factor. *The Journal of Cell Biology.*
460 **100** (4), 1219–1227 (1985).
461   10.   Buckley, A., Davidson, J. M., Kamerath, C. D., Wolt, T. B., Woodward, S. C. Sustained
462 release of epidermal growth factor accelerates wound repair. *Proceedings of the National*
463 *Academy of Sciences.* **82** (21), 7340–7344 (1985).
464   11.   Peterson, J. M., Barbul, A., Breslin, R. J., Wasserkrug, H. L., Efron, G. Significance of T-
465 lymphocytes in wound healing. *Surgery.* **102** (2), 300–305 (1987).
466   12.   Efron, J. E., Frankel, H. L., Lazarou, S. A., Wasserkrug, H. L., Barbul, A. Wound healing and
467 T-lymphocytes. *Journal of Surgical Research.* **48** (5), 460–463 (1990).
468   13.   Schäffer, M. R., Tantry, U., Thornton, F. J., Barbul, A. Inhibition of nitric oxide synthesis in
469 wounds: pharmacology and effect on accumulation of collagen in wounds in mice. *The*
470 *European Journal of Surgery = Acta Chirurgica.* **165** (3), 262–267 (1999).
471   14.   Opalenik, S. R., Davidson, J. M. Fibroblast differentiation of bone marrow-derived cells
472 during wound repair. *FASEB Journal: Official Publication of the Federation of American Societies*
473 *for Experimental Biology.* **19** (11), 1561–1563 (2005).
474   15.   Järveläinen, H. et al. A role for decorin in cutaneous wound healing and angiogenesis.
475 *Wound Repair and Regeneration: Official Publication of the Wound Healing Society [and] the*
476 *European Tissue Repair Society.* **14** (4), 443–452 (2006).
477   16.   Luckett, L. R., Gallucci, R. M. Interleukin-6 (IL-6) modulates migration and matrix
478 metalloproteinase function in dermal fibroblasts from IL-6KO mice. *The British Journal of*
479 *Dermatology.* **156** (6), 1163–1171 (2007).
480   17.   Daniel, T. et al. Regulation of the postburn wound inflammatory response by
481 gammadelta T-cells. *Shock.* **28** (3), 278–283 (2007).
482   18.   MacLauchlan, S. et al. Macrophage fusion, giant cell formation, and the foreign body
483 response require matrix metalloproteinase 9. *Journal of Leukocyte Biology.* **85** (4), 617–626
484 (2009).

485   19.   Schwacha, M. G., Thobe, B. M., Daniel, T., Hubbard, W. J. Impact of thermal injury on
486   wound infiltration and the dermal inflammatory response. *Journal of Surgical Research.* **158** (1),
487   112–120 (2010).
488   20.   Ganesh, K. et al. Prostaglandin E2 Induces Oncostatin M Expression in Human Chronic
489   Wound Macrophages through Axl Receptor Tyrosine Kinase Pathway. *The Journal of*
490   *Immunology.* **189** (5), 2563–2573 (2012).
491   21.   Deskins, D. L. et al. Human mesenchymal stromal cells: identifying assays to predict
492   potency for therapeutic selection. *Stem Cells Translational Medicine.* **2** (2), 151–158 (2013).
493   22.   Daley, J. M., Brancato, S. K., Thomay, A. A., Reichner, J. S, Albina, J. E. The phenotype of
494   murine wound macrophages. *Journal of Leukocyte Biology.* **87** (1), 59–67 (2010).
495   23.   Thomay, A. A. et al. Disruption of Interleukin-1 Signaling Improves the Quality of Wound
496   Healing. *The American Journal of Pathology.* **174** (6), 2129–2136 (2009).
497   24.   Brancato, S. K. et al. Toll-like receptor 4 signaling regulates the acute local inflammatory
498   response to injury and the fibrosis/neovascularization of sterile wounds. *Wound Repair and*
499   *Regeneration: Official Publication of the Wound Healing Society [and] the European Tissue*
500   *Repair Society.* **21** (4), 624–633 (2013).
501   25.   Daley, J. M. et al. Modulation of macrophage phenotype by soluble product(s) released
502   from neutrophils. *Journal of Immunology*. **174** (4), 2265–2272 (2005).
503   26.   Crane, M. J. et al. The monocyte to macrophage transition in the murine sterile wound.
504   *PloS One* **9** (1), e86660 (2014).
505   27.   Falanga, V. et al. Full-thickness wounding of the mouse tail as a model for delayed wound
506   healing: accelerated wound closure in Smad3 knock-out mice. *Wound Repair and Regeneration.*
507   **12** (3), 320–326 (2004).
508   28.   Li, J. et al. Molecular mechanisms underlying skeletal growth arrest by cutaneous
509   scarring. *Bone.* **66**, 223–231 (2014).
510   29.   Zhou, S. et al. A Novel Model for Cutaneous Wound Healing and Scarring in the Rat.
511   *Plastic and Reconstructive Surgery.* **143** (2), 468-477 (2019).
512   30.   Crane, M. J. et al. Pulmonary influenza A virus infection leads to suppression of the
513   innate immune response to dermal injury. *PLOS Pathogens.* **14** (8), e1007212 (2018).
514   31.   Grada, A., Mervis, J., Falanga, V. Research Techniques Made Simple: Animal
515   Models of Wound Healing. *Journal of Investigative Dermatology.* **138** (10), 2095–2105.e1
516   (2018).
517   32.   Rittié, L. Cellular mechanisms of skin repair in humans and other mammals. *Journal of*
518   *Cell Communication and Signaling.* **10** (2), 103–120 (2016).
519   33.   Falanga, V. et al. Autologous Bone Marrow–Derived Cultured Mesenchymal Stem Cells
520   Delivered in a Fibrin Spray Accelerate Healing in Murine and Human Cutaneous Wounds. *Tissue*
521   *Engineering.* **13** (6), 1299–1312 (2007).
522   34.   Lucas, T. et al. Differential Roles of Macrophages in Diverse Phases of Skin Repair. *The*
523   *Journal of Immunology.* **184** (7), 3964–3977 (2010).
524   35.   Wang, J. et al. Visualizing the function and fate of neutrophils in sterile injury and repair.
525   *Science.* **358** (6359), 111–116 (2017).
526   36.   Mirza, R. E., Koh, T. J. Contributions of cell subsets to cytokine production during normal
527   and impaired wound healing. *Cytokine*. 1–4 (2014).
528   37.   Mirza, R., DiPietro, L. A., Koh, T. J. Selective and Specific Macrophage Ablation Is

Detrimental to Wound Healing in Mice. *The American Journal of Pathology.* **175** (6), 2454–2462 (2010).

38.   DiPietro, L. A., Burdick, M., Low, Q. E., Kunkel, S. L., Strieter, R. M. MIP-1alpha as a critical macrophage chemoattractant in murine wound repair. *Journal of Clinical Investigation.* **101** (8), 1693–1698 (1998).

39.   Wetzler, C., Kämpfer, H., Stallmeyer, B., Pfeilschifter, J., Frank, S. Large and Sustained Induction of Chemokines during Impaired Wound Healing in the Genetically Diabetic Mouse: Prolonged Persistence of Neutrophils and Macrophages during the Late Phase of Repair. *Journal of Investigative Dermatology.* **115** (2), 245–253 (2000).

40.   Kim, D. J., Mustoe, T., Clark, R. A. Cutaneous wound healing in aging small mammals: a systematic review. *Wound Repair and Regeneration.* **23** (3), 318–339 (2015).
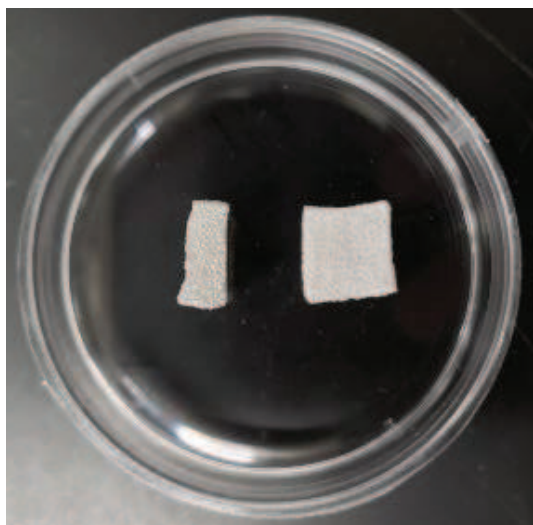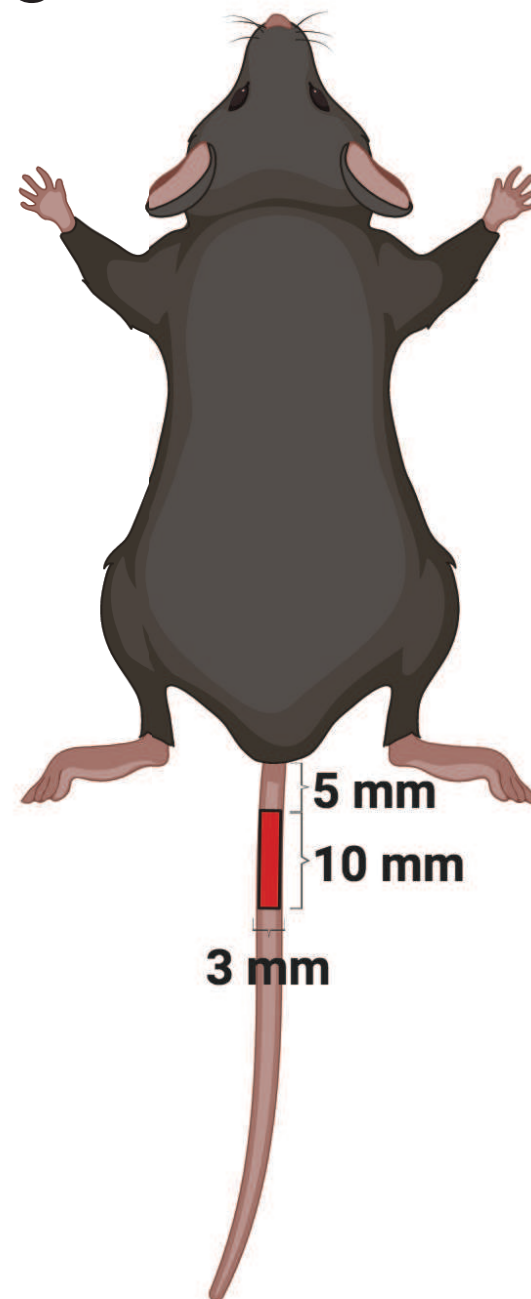
Figure 1

Figure 2

Figure 3
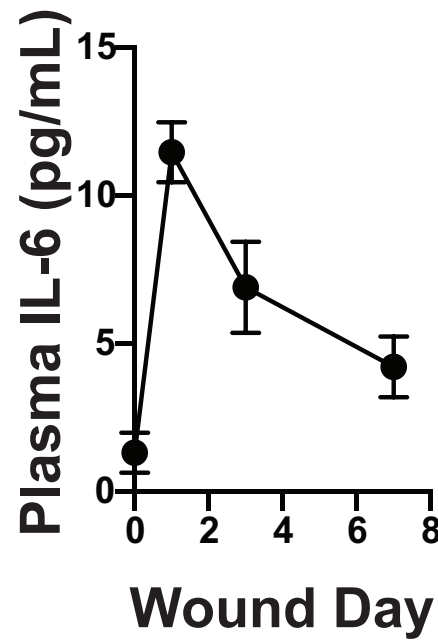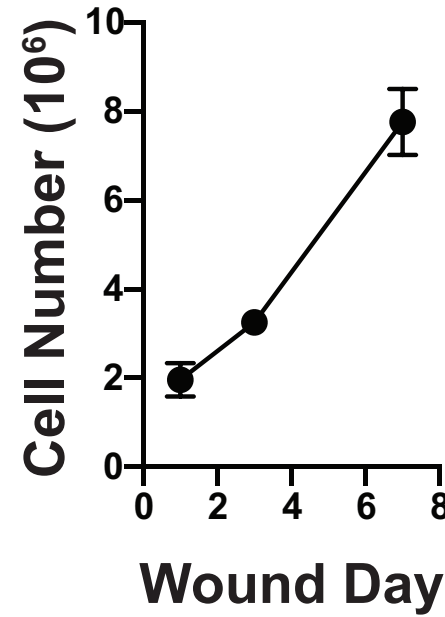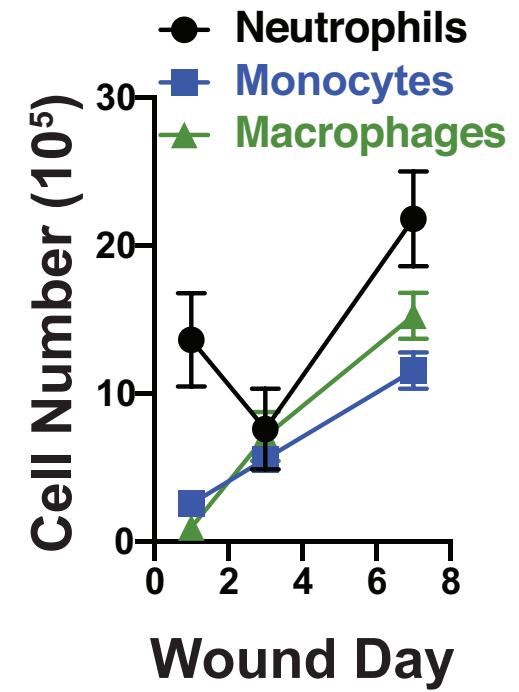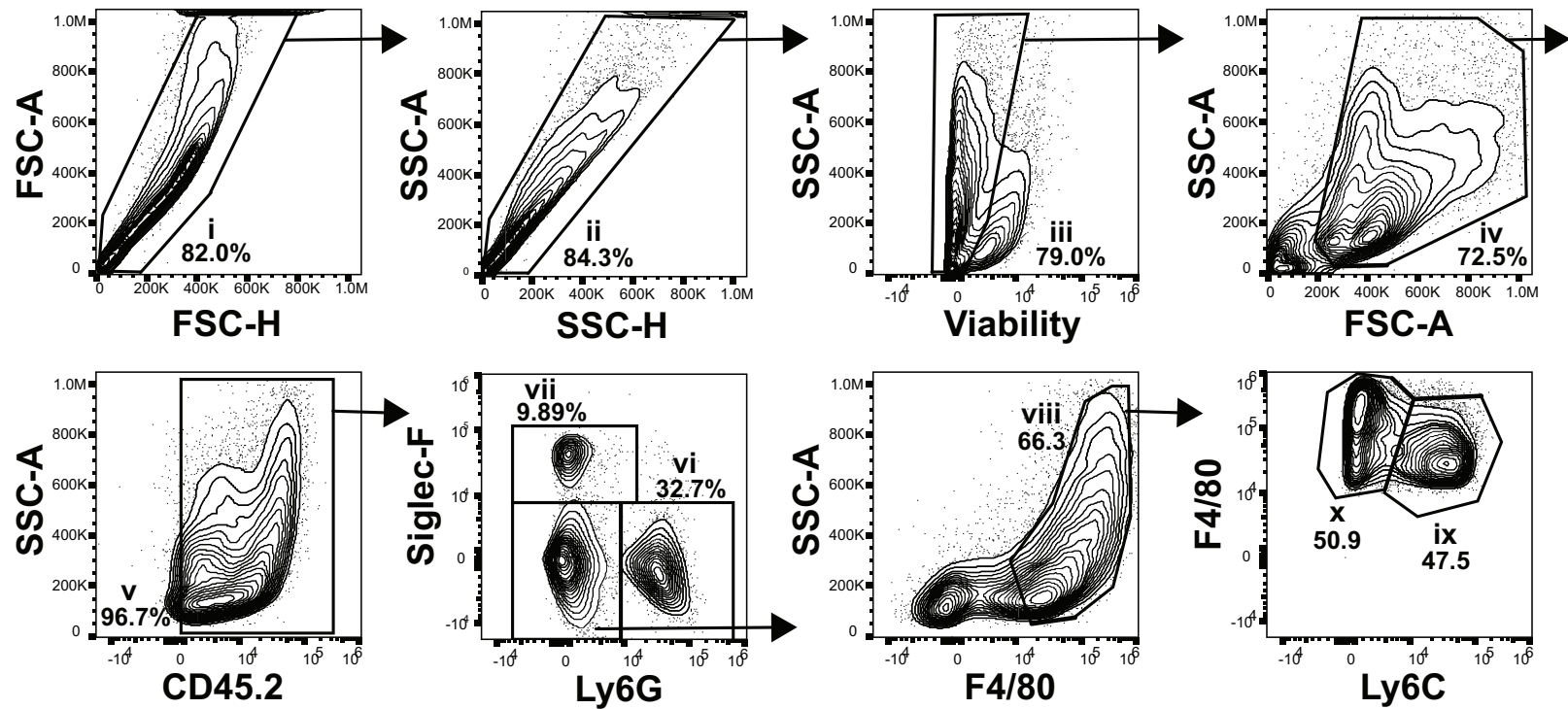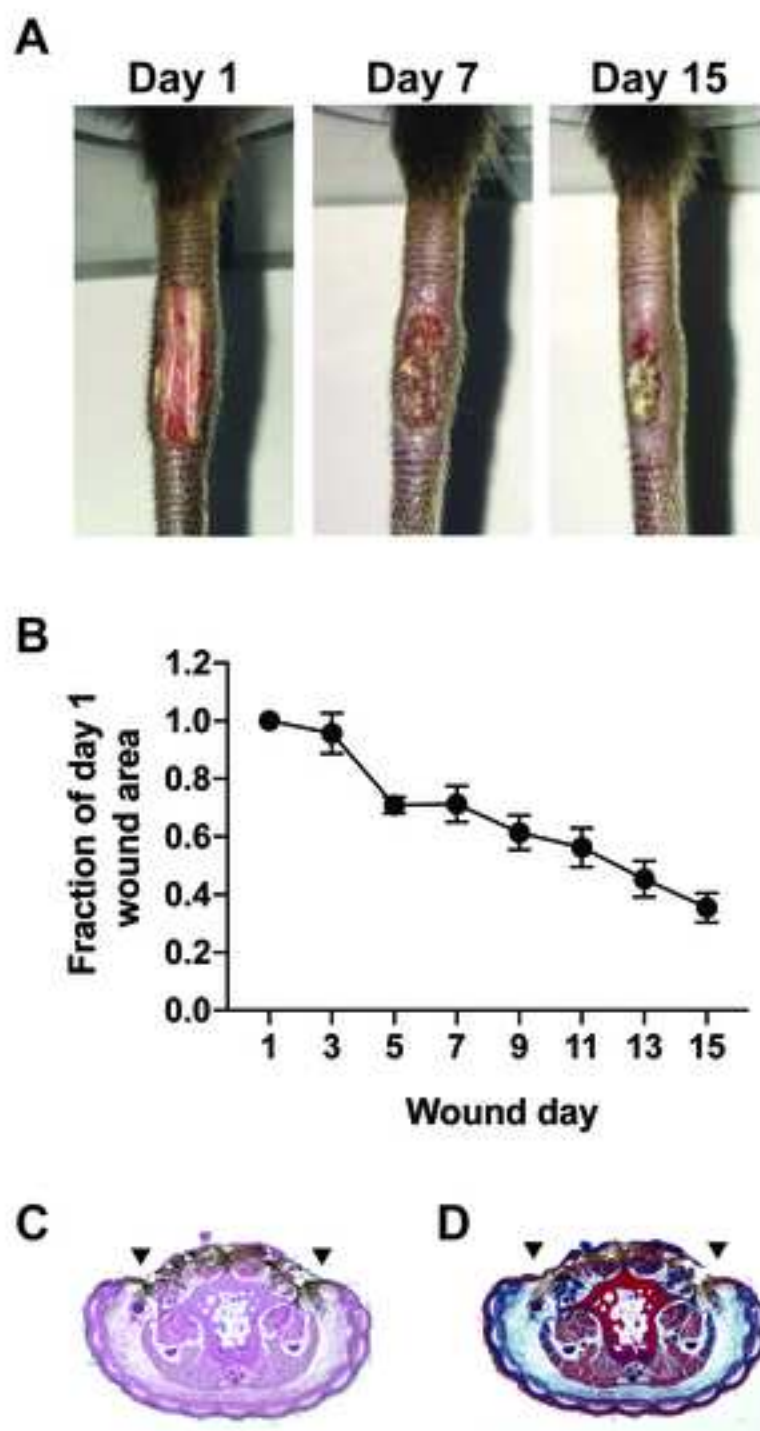
Name of Material/Equipment	Company	Catalog Number	Comments/Description
10x Phosphate Buffered Saline	Fisher Scientific	BP3991	
15 mL centrifuge tubes, Olympus	Genesee	28-103	
1x HBSS (+Calcium, +Magnesium, –Phenol Red)	ThermoFisher Scientific	14025076	
5ml Syringe	BD	309646	
Anti-mouse CD45.2-APC Fire750	BioLegend	109852	Clone 104
Anti-mouse F4/80-eFluor660	ThermoFisher Scientific	50-4801-82	Clone BM8
Anti-mouse Ly6C-FITC	BD Biosciences	553104	Clone AL-21
Anti-mouse Ly6G-PerCP-eFluor710	ThermoFisher Scientific	46-9668-82	Clone 1A8-Ly6g
Anti-mouse Siglec-F-APC-R700	BD Biosciences	565183	Clone E50-2440
Autoclip Stainless Steel Wound Clip Applier	Braintree Scientific	NC9021392	
Autoclip Stainless Steel Wound Clips, 9mm	Braintree Scientific	NC9334081	
Blender Bag, 80mL	Fisher Scientific	14258201	
Culture Tube, 16mL, 17x100	Genesee Scientific	21-130	
Fetal Bovine Serum - Standard	ThermoFisher Scientific	10437028	
Fixable Viability Dye eFluor506	ThermoFisher Scientific	65-0866-14	
Hepes Solution, 1M	Genesee Scientific	25-534	
ImageJ Software	NIH		
Penicillin-Streptomycin (5000 U/mL)	ThermoFisher Scientific	15070-063	
Polyvinyl alcohol sponge - large pore size	Ivalon/PVA Unlimited		www.sponge-pva.com
Povidone-iodine solution, 10%	Fisher Scientific	3955-16	

Spray barrier film, Cavilon	3M	3346E
Stomacher 80 Biomaster, 110V	Seward	0080/000/AJ

Amanda Jamieson

Division of Biology & Medicine

Molecular Microbiology & Immunology

Providence, RI 02912

Tel: 401-863-9775

Email: amanda_jamieson@brown.edu

November 22nd, 2019

Dear Editors:

Enclosed please find our manuscript entitled "Assessment of acute wound healing using the dorsal subcutaneous polyvinyl alcohol sponge implantation and excisional tail skin wound models" by Crane *et al*, which we are resubmitting for consideration for publication. We have clarified several points and made updates in response to the reviewer and editor comments. These additions greatly improve the manuscript. The purpose of this manuscript is to give detailed descriptions on how to perform these procedures so that other researchers who are interested in studying several aspects of wound healing can use them. The helpful comments from the reviewers has helped us achieve this aim.

Wound healing is a complex process that requires the orderly progression of inflammation, granulation tissue formation, fibrosis, and resolution. Murine models provide valuable mechanistic insight into these processes; however, no single model fully addresses all aspects of the wound healing response, and there are caveats with all of the models. Instead, it is ideal to use complementary models to address the different aspects of wound healing. This manuscript describes two distinct models that allow us to measure both the wound healing rate and the immune response to healing wounds.

Here, two complementary surgical wound models are described, one of which elucidates early acute cellular and cytokine wound healing responses, and the other of which allows for the assessment of wound closure over time as well as histological analyses. The dorsal subcutaneous implantation of polyvinyl alcohol (PVA) sponges allows for the retrieval of cytokine-rich wound fluids and cellular infiltrates. The rate of wound closure is determined using a tail skin excision model. This approach offers certain advantages over the dorsal skin punch biopsy method, such as a slower wound closure rate and also ease of visualization.

A point by point comment on the reviewer and editorial comments follows.

Editorial comments:

Changes to be made by the Author(s):

1. Please take this opportunity to thoroughly proofread the manuscript to ensure that there are no

spelling or grammar issues. The JoVE editor will not copy-edit your manuscript and any errors in the submitted revision may be present in the published version.

2. Please remove all commercial language from your manuscript and use generic terms instead. All commercial products should be sufficiently referenced in the Table of Materials and Reagents. For example: Stomacher, LegendPlex, BioRender.com, etc.

Commercial language has bee removed from the manuscript.

3. Please ensure that all text in the protocol section is written in the imperative tense as if telling someone how to do the technique (e.g., "Do this," "Ensure that," etc.). The actions should be described in the imperative tense in complete sentences wherever possible. Avoid usage of phrases such as "could be," "should be," and "would be" throughout the Protocol. Any text that cannot be written in the imperative tense may be added as a "Note."

The protocol language has been adjusted and now reads in the imperative tense.

4. Please add more details to your protocol steps. Please ensure you answer the "how" question, i.e., how is the step performed?

More details have been added to many of the protocol steps. These include more information about the mice and anesthesia procedures, as requested. The methods of sponge placement and cell isolation has been expanded. The antibody staining protocol now also includes more specific instruction.

5. 2.2, 5.1: Please include strain, age, sex of the mouse used for the study? How is the anesthesia step performed? Do you check the mouse for the lack of pedal reflex?

This information has been added to the protocol.

6. 2.5: How do you place the sponges? What are the controls in this case?

More detail was added to this aspect of the protocol, as stated above. In this model system, sham surgery or other controls are not informative, so have not been included.

 7. 3.2: Please include the euthanasia method. After how many days do you perform step 3?
The euthanasia method has been updated and duration of the experiment has been added

 8. 4.3: Please include the volume of the HBSS used.

The volume of HBSS is 5mL, as stated in the protocol

  9. 4.5: How is the stomaching performed? Please include button clicks, knob turns etc.

More detail has been added to this section of the protocol.

10. 6.2: What is the blocking antibody in your experiment?

The blocking antibody is the anti-CD16/CD32 FCgammaRII/III, as stated in the protocol and materials spreadsheet.

11. There is a 10-page limit for the Protocol, but there is a 2.75-page limit for filmable content. Please highlight 2.75 pages or less of the Protocol (including headings and spacing) that identifies the essential steps of the protocol for the video, i.e., the steps that should be visualized to tell the most cohesive story of the Protocol. 12. Please obtain explicit copyright permission to reuse any figures from a previous publication. Explicit permission can be expressed in the form of a letter from the editor or a link to the editorial policy that allows re-prints. Please upload this information as a .doc or .docx file to your Editorial Manager account. The Figure must be cited appropriately in the Figure Legend, i.e. "This figure has been modified from [citation]."

Filmable content is highlighted in yellow. No figures are reused from published content.

Reviewers' comments:

Reviewer #1:

Manuscript Summary: Crane et al report on the broad assessment of acute wound healing using the dorsal subcutaneous polyvinyl alcohol sponge implantation and excisional tail skin wound models. There are two models addressed here: (1) PVA sponge model (2) excisional tail skin model. PVA sponge is used by numerous laboratories and is of broad interest. The tail skin model has little relevance to wound healing and it is understandable that this group finds it useful but it is certainly not of broad interest. Specific comments are listed below:

1. Focus the manuscript on the PVA sponge model

The tail wound model has been kept in the manuscript; however, it is now the last section of the protocol and is only presented in the context of planimetric analysis. Further applications of the model are discussed in the introduction and the discussion, with appropriate citations.

2. As it relates to experimental models, numerous works have highlighted limitations of the murine models - although we all use it - as opposed to porcine models (higher concordance with human wounds). In the interest of rigor such limitations should be candidly discussed.

The authors agree that the murine models possess several limitations, and text has been added to both the introduction and discussion to present these limitations in addition to the advantages of

the murine system.

3. Late stage repair: tail wound model is not widely accepted and therefore not of broad interest. Should late stage be of interest, scar remodeling over many weeks should be addressed

The tail wound model is now presented only in the context of providing an alternative skin site in which to measure the rate of wound repair.

4. "These latter methods typically require enzymatic digestion of the dermal tissue and result in low cellular yields": show comparative data to support claim

This text has been removed from the manuscript.

5. Sponge model: appropriately cite published work employing this model to study wound sciences. This will help support the case of broad interest

Additional citations have been included throughout the manuscript.

Overall, the sponge piece is an interesting contribution that would benefit from some revision.

Reviewer #2:

Manuscript Summary: This is a methodology manuscript that describe two models of wound healing. The tail model of wound healing of wound healing to look at the re epithelialization and wound closure. The PVA sponge model to look at the inflammatory response.

Major Concerns: Why do the authors consider the study as broad assessment?

The authors acknowledge that there are other aspects of wound repair not covered by these models, and so this language has been removed from the title.

So .... What is the aspect of comparisons in the two model? Not clear what is the point of the study comparing two models of wound healing which are two completely different models as the author discussed. In this study, each model was handled differently. PVA model was used to assess the inflammatory response. The tail model of wound healing was used to measure wound closure. It would be interesting running the same testes on the two model to be comparable.

When studying the effect of a co-morbid condition on wound repair, such as post-operative pneumonia (as referenced in the manuscript) the PVA sponge model is limited because it cannot provide information on the rate of healing. In these cases, it is helpful to take multiple approaches to gain a more complete dataset on wound healing defects. So, while not directly comparable, the authors believe that the two models can be used in concert to examine various aspects of the wound healing response. The text of the introduction and discussion has been modified to reflect this.

The study on the tail model of wound healing here is very limited and not well described.

More details of the experimental procedure have been added to this section.

tail model of wound healing of wound healing: Why would the author choose tail as the site of injury? how would this be different from the well-known dermal wound healing model in which the incision was done on the dorsum of the animals.

Why do the authors choose the tail? better to choose area that histologically and anatomically resemble human models such as the dorsum of the animals. For the best of our knowledges the tail structure does not resemble human.

The tail model is presented as an alternative to the dorsal punch biopsy model; distinctions between the two models are more fully discussed in the introduction and the discussion. According to the literature, both the dorsal skin and tail skin on mice have benefits and limitations to modeling human skin, and a discussion of this has been added to the text.

Tail as a site of expert: There would be variability in the result. the animal behaviour would affect the results. Hyperkinetic animals with movement of the tail would affect the healing. It would be better choosing an animal model that resembling human.

The potential for this model is acknowledged in the discussion; solo housing is recommended, especially for aggressive strains or male mice. The authors believe this could be a concern with any dermal injury, regardless of location.

The author would better investigate the tail model of wound healing in more details by looking at the histopathological changes, inflammatory changes etc and show how was the responses different in the two model. The author considers the tail model of wound healing as a good model for re epithelialization than dermal wound healing. It would be important to characterize re epithelialization in both models or at least in the tail model of wound healing . This would be by showing epidermal changes over time course, by immunostaining using keratinocyte marker, Ki67 ...etc. this would be done over time course.

The authors agree that these experiments would provide valuable insight into the model, but feel that it is outside of the scope of this manuscript. Citations have been included for other studies that have addressed some of these aspects.

Most of the points the author stressed on in the PVA sponge model, already studied before. Nothing new in the authors' finding. PVA model is a well established model of wound healing, that has been used for decade. it got the advantage which the author covered very well and limitations.

The authors agree that this is a widely used, well-understood model. The goal of this protocol is

to provide a visual guide to the surgery and some downstream applications for researchers new to the system.

Minor Concerns:

Technical in Materials and Methods: Number of animals used. Animal age weight. Details of animal termination, not enough to say according to...... etc

These details have been updated. The number of animals used in representative experiments is indicated in the figure legends.

Source of the sponge. Criteria of the sponge. photo of the collected sponge at the end of the experiments at different time point, weight, gender, species stain. Etc

The source of the sponge material is included in the table of materials.

Tail is different and got cartilage and dense CT which might need special treatment to soften the tissue before sectioning. This was not covered in material and method. Could the author show photos of the wounds at different time points. This would provide a good understanding of the re epithelialization and scarring

Histological analysis has been removed from the protocol. Images of the tail wound at days 1, 7, and 15 are shown in Figure 3. Figure 1 has been amended to now include images of wound fluid and sponges isolated from day seven wounds.

Immunostaining: The author done immunostaining for different inflammatory cells. why there is no images showing the finding. this would be important showing different cell types morphologically. The concentration of the antibodies used is missed

Figure 2 shows representative flow cytometry analysis of cells isolated from PVA sponge wounds. The protocol has been updated with the concentration of antibodies used for the immunostaining.

Reviewer #3: This manuscript can originate a useful guideline for those that are starting to study cutaneous healing.

Reviewer #4:

Manuscript Summary: The manuscript list two different wound healing models in mice of different parts of the wound healing process. The protocol is well written, and can be followed in detail.

Major Concerns: It might not have been the focus of the authors, but the reviewer is not able to find sth. really new in this description. The tail model seems not to be the most elucidating wound healing model in my eyes. There are better ones!

The authors intended to convey the tail wound model as a tractable system that provides a slower-healing alternative to some dorsal punch biopsies. The text has been updated to reflect this intent.

Thank you for your consideration.

Best regards,

Amanda M. Jamieson Ph.D

Assistant Professor
Brown University

jove
JOURNAL OF VISUALIZED EXPERIMENTS

1 Alewife Center #200
Cambridge, MA 02140
tel. 617.945.9051
www.jove.com

ARTICLE AND VIDEO LICENSE AGREEMENT

Title of Article:	Broad assessment of acute wound healing using the dorsal subcutaneous polyvinyl alcohol sponge implantation and excisional tail skin wound models
Author(s):	Meredith J. Crane, William L. Henry, Jr., Holly L. Tran, Jorge E. Albina, Amanda M. Jamieson

Item 1: The Author elects to have the Materials be made available (as described at http://www.jove.com/publish) via:

☐ Standard Access   ☑ Open Access

Item 2: Please select one of the following items:

☑ The Author is **NOT** a United States government employee.

☐ The Author is a United States government employee and the Materials were prepared in the course of his or her duties as a United States government employee.

☐ The Author is a United States government employee but the Materials were NOT prepared in the course of his or her duties as a United States government employee.

ARTICLE AND VIDEO LICENSE AGREEMENT

1.   **Defined Terms.** As used in this Article and Video License Agreement, the following terms shall have the following meanings: "**Agreement**" means this Article and Video License Agreement; "**Article**" means the article specified on the last page of this Agreement, including any associated materials such as texts, figures, tables, artwork, abstracts, or summaries contained therein; "**Author**" means the author who is a signatory to this Agreement; "**Collective Work**" means a work, such as a periodical issue, anthology or encyclopedia, in which the Materials in their entirety in unmodified form, along with a number of other contributions, constituting separate and independent works in themselves, are assembled into a collective whole; "**CRC License**" means the Creative Commons Attribution-Non Commercial-No Derivs 3.0 Unported Agreement, the terms and conditions of which can be found at: http://creativecommons.org/licenses/by-nc-nd/3.0/legalcode; "**Derivative Work**" means a work based upon the Materials or upon the Materials and other pre-existing works, such as a translation, musical arrangement, dramatization, fictionalization, motion picture version, sound recording, art reproduction, abridgment, condensation, or any other form in which the Materials may be recast, transformed, or adapted; "**Institution**" means the institution, listed on the last page of this Agreement, by which the Author was employed at the time of the creation of the Materials; "**JoVE**" means MyJove Corporation, a Massachusetts corporation and the publisher of The Journal of Visualized Experiments; "**Materials**" means the Article and / or the Video; "**Parties**" means the Author and JoVE; "**Video**" means any video(s) made by the Author, alone or in conjunction with any other parties, or by JoVE or its affiliates or agents, individually or in collaboration with the Author or any other parties, incorporating all or any portion of the Article, and in which the Author may or may not appear.

2.   **Background.** The Author, who is the author of the Article, in order to ensure the dissemination and protection of the Article, desires to have the JoVE publish the Article and create and transmit videos based on the Article. In furtherance of such goals, the Parties desire to memorialize in this Agreement the respective rights of each Party in and to the Article and the Video.

3.   **Grant of Rights in Article.** In consideration of JoVE agreeing to publish the Article, the Author hereby grants to JoVE, subject to **Sections 4** and **7** below, the exclusive, royalty-free, perpetual (for the full term of copyright in the Article, including any extensions thereto) license (a) to publish, reproduce, distribute, display and store the Article in all forms, formats and media whether now known or hereafter developed (including without limitation in print, digital and electronic form) throughout the world, (b) to translate the Article into other languages, create adaptations, summaries or extracts of the Article or other Derivative Works (including, without limitation, the Video) or Collective Works based on all or any portion of the Article and exercise all of the rights set forth in (a) above in such translations, adaptations, summaries, extracts, Derivative Works or Collective Works and (c) to license others to do any or all of the above. The foregoing rights may be exercised in all media and formats, whether now known or hereafter devised, and include the right to make such modifications as are technically necessary to exercise the rights in other media and formats. If the "Open Access" box has been checked in **Item 1** above, JoVE and the Author hereby grant to the public all such rights in the Article as provided in, but subject to all limitations and requirements set forth in, the CRC License.

612542.6   For questions, please contact us at submissions@jove.com or +1.617.945.9051.

4. **Retention of Rights in Article.** Notwithstanding the exclusive license granted to JoVE in **Section 3** above, the Author shall, with respect to the Article, retain the non-exclusive right to use all or part of the Article for the non-commercial purpose of giving lectures, presentations or teaching classes, and to post a copy of the Article on the Institution's website or the Author's personal website, in each case provided that a link to the Article on the JoVE website is provided and notice of JoVE's copyright in the Article is included. All non-copyright intellectual property rights in and to the Article, such as patent rights, shall remain with the Author.

5. **Grant of Rights in Video – Standard Access.** This **Section 5** applies if the "Standard Access" box has been checked in **Item 1** above or if no box has been checked in **Item 1** above. In consideration of JoVE agreeing to produce, display or otherwise assist with the Video, the Author hereby acknowledges and agrees that, Subject to **Section 7** below, JoVE is and shall be the sole and exclusive owner of all rights of any nature, including, without limitation, all copyrights, in and to the Video. To the extent that, by law, the Author is deemed, now or at any time in the future, to have any rights of any nature in or to the Video, the Author hereby disclaims all such rights and transfers all such rights to JoVE.

6. **Grant of Rights in Video – Open Access.** This **Section 6** applies only if the "Open Access" box has been checked in **Item 1** above. In consideration of JoVE agreeing to produce, display or otherwise assist with the Video, the Author hereby grants to JoVE, subject to **Section 7** below, the exclusive, royalty-free, perpetual (for the full term of copyright in the Article, including any extensions thereto) license (a) to publish, reproduce, distribute, display and store the Video in all forms, formats and media whether now known or hereafter developed (including without limitation in print, digital and electronic form) throughout the world, (b) to translate the Video into other languages, create adaptations, summaries or extracts of the Video or other Derivative Works or Collective Works based on all or any portion of the Video and exercise all of the rights set forth in (a) above in such translations, adaptations, summaries, extracts, Derivative Works or Collective Works and (c) to license others to do any or all of the above. The foregoing rights may be exercised in all media and formats, whether now known or hereafter devised, and include the right to make such modifications as are technically necessary to exercise the rights in other media and formats. For any Video to which this **Section 6** is applicable, JoVE and the Author hereby grant to the public all such rights in the Video as provided in, but subject to all limitations and requirements set forth in, the CRC License.

7. **Government Employees.** If the Author is a United States government employee and the Article was prepared in the course of his or her duties as a United States government employee, as indicated in **Item 2** above, and any of the licenses or grants granted by the Author hereunder exceed the scope of the 17 U.S.C. 403, then the rights granted hereunder shall be limited to the maximum rights permitted under such statute. In such case, all provisions contained herein that are not in conflict with such statute shall remain in full force and effect, and all provisions contained herein that do so conflict shall be deemed to be amended so as to provide to JoVE the maximum rights permissible within such statute.

8. **Protection of the Work.** The Author(s) authorize JoVE to take steps in the Author(s) name and on their behalf if JoVE believes some third party could be infringing or might infringe the copyright of either the Author's Article and/or Video.

9. **Likeness, Privacy, Personality.** The Author hereby grants JoVE the right to use the Author's name, voice, likeness, picture, photograph, image, biography and performance in any way, commercial or otherwise, in connection with the Materials and the sale, promotion and distribution thereof. The Author hereby waives any and all rights he or she may have, relating to his or her appearance in the Video or otherwise relating to the Materials, under all applicable privacy, likeness, personality or similar laws.

10. **Author Warranties.** The Author represents and warrants that the Article is original, that it has not been published, that the copyright interest is owned by the Author (or, if more than one author is listed at the beginning of this Agreement, by such authors collectively) and has not been assigned, licensed, or otherwise transferred to any other party. The Author represents and warrants that the author(s) listed at the top of this Agreement are the only authors of the Materials. If more than one author is listed at the top of this Agreement and if any such author has not entered into a separate Article and Video License Agreement with JoVE relating to the Materials, the Author represents and warrants that the Author has been authorized by each of the other such authors to execute this Agreement on his or her behalf and to bind him or her with respect to the terms of this Agreement as if each of them had been a party hereto as an Author. The Author warrants that the use, reproduction, distribution, public or private performance or display, and/or modification of all or any portion of the Materials does not and will not violate, infringe and/or misappropriate the patent, trademark, intellectual property or other rights of any third party. The Author represents and warrants that it has and will continue to comply with all government, institutional and other regulations, including, without limitation all institutional, laboratory, hospital, ethical, human and animal treatment, privacy, and all other rules, regulations, laws, procedures or guidelines, applicable to the Materials, and that all research involving human and animal subjects has been approved by the Author's relevant institutional review board.

11. **JoVE Discretion.** If the Author requests the assistance of JoVE in producing the Video in the Author's facility, the Author shall ensure that the presence of JoVE employees, agents or independent contractors is in accordance with the relevant regulations of the Author's institution. If more than one author is listed at the beginning of this Agreement, JoVE may, in its sole

612542.6   For questions, please contact us at submissions@jove.com or +1.617.945.9051.

![JoVE logo] 1 Alewife Center #200
Cambridge, MA 02140
tel. 617.945.9051
www.jove.com

VISUALIZED EXPERIMENTS
JOURNAL OF

ARTICLE AND VIDEO LICENSE AGREEMENT

discretion, elect not take any action with respect to the Article until such time as it has received complete, executed Article and Video License Agreements from each such author. JoVE reserves the right, in its absolute and sole discretion and without giving any reason therefore, to accept or decline any work submitted to JoVE. JoVE and its employees, agents and independent contractors shall have full, unfettered access to the facilities of the Author or of the Author's institution as necessary to make the Video, whether actually published or not. JoVE has sole discretion as to the method of making and publishing the Materials, including, without limitation, to all decisions regarding editing, lighting, filming, timing of publication, if any, length, quality, content and the like.

12.   **Indemnification.** The Author agrees to indemnify JoVE and/or its successors and assigns from and against any and all claims, costs, and expenses, including attorney's fees, arising out of any breach of any warranty or other representations contained herein. The Author further agrees to indemnify and hold harmless JoVE from and against any and all claims, costs, and expenses, including attorney's fees, resulting from the breach by the Author of any representation or warranty contained herein or from allegations or instances of violation of intellectual property rights, damage to the Author's or the Author's institution's facilities, fraud, libel, defamation, research, equipment, experiments, property damage, personal injury, violations of institutional, laboratory, hospital, ethical, human and animal treatment, privacy or other rules, regulations, laws, procedures or guidelines, liabilities and other losses or damages related in any way to the submission of work to JoVE, making of videos by JoVE, or publication in JoVE or elsewhere by JoVE. The Author shall be responsible for, and shall hold JoVE harmless from, damages caused by lack of sterilization, lack of cleanliness or by contamination due to

the making of a video by JoVE its employees, agents or independent contractors. All sterilization, cleanliness or decontamination procedures shall be solely the responsibility of the Author and shall be undertaken at the Author's expense. All indemnifications provided herein shall include JoVE's attorney's fees and costs related to said losses or damages. Such indemnification and holding harmless shall include such losses or damages incurred by, or in connection with, acts or omissions of JoVE, its employees, agents or independent contractors.

13.   **Fees.** To cover the cost incurred for publication, JoVE must receive payment before production and publication of the Materials. Payment is due in 21 days of invoice. Should the Materials not be published due to an editorial or production decision, these funds will be returned to the Author. Withdrawal by the Author of any submitted Materials after final peer review approval will result in a US$1,200 fee to cover pre-production expenses incurred by JoVE. If payment is not received by the completion of filming, production and publication of the Materials will be suspended until payment is received.

14.   **Transfer, Governing Law.** This Agreement may be assigned by JoVE and shall inure to the benefits of any of JoVE's successors and assignees. This Agreement shall be governed and construed by the internal laws of the Commonwealth of Massachusetts without giving effect to any conflict of law provision thereunder. This Agreement may be executed in counterparts, each of which shall be deemed an original, but all of which together shall be deemed to me one and the same agreement. A signed copy of this Agreement delivered by facsimile, e-mail or other means of electronic transmission shall be deemed to have the same legal effect as delivery of an original signed copy of this Agreement.

A signed copy of this document must be sent with all new submissions. Only one Agreement is required per submission.

CORRESPONDING AUTHOR

Name: Amanda Jamieson

Department: Molecular Microbiology and Immunology

Institution: Brown University

Title: Assistant Professor

Signature: *Amanda Jamieson*   Date: 08/08/2019

Please submit a **signed** and **dated** copy of this license by one of the following three methods:
1. Upload an electronic version on the JoVE submission site
2. Fax the document to +1.866.381.2236
3. Mail the document to JoVE / Attn: JoVE Editorial / 1 Alewife Center #200 / Cambridge, MA 02140

612542.6   For questions, please contact us at submissions@jove.com or +1.617.945.9051.

Signature Certificate

Document Ref.: PYQK9-DJHU8-SMFVT-DBMRQ

Document signed by:

Amanda Jamieson

Verified E-mail:
amanda_jamieson@brown.edu

Amanda Jamieson

IP: 128.148.231.12 | Date: 08 Aug 2019 15:28:50 UTC

Document completed by all parties on:
08 Aug 2019 15:28:50 UTC

Page 1 of 1

Signed with **PandaDoc.com**

PandaDoc is the document platform that boosts your company's revenue by accelerating the way it transacts.